Technology in Cancer Research and Treatment
ISSN 1533-0346
Volume 6, Number 4, August 2007

Technical Description, Phantom Accuracy, and Clinical Feasibility for Single-session Lung Radiosurgery Using Robotic Image-guided Real-time Respiratory Tumor Tracking

www.tcrt.org

A. Muacevic, M.D.[1,*]
C. Drexler, M.Sc.[1]
B. Wowra, M.D.[1]
A. Schweikard, Ph.D.[2]
A. Schlaefer, Ph.D.[2]
R. T. Hoffmann, M.D.[3]
R. Wilkowski, M.D.[4]
H. Winter, M.D.[5]
M. Reiser, M.D.[3]

[1]European Cyberknife Center
Munich Grosshadern
Munich, Germany
[2]Institute of Robotics and Cognitive Systems University
Luebeck, Germany
[3]Institute of Clinical Radiology
University of Munich Hospital
Germany
[4]Department of Radiation Oncology
Bad Trissl Hospital
Germany
[5]Department of Thoracic Surgery
University of Munich Hospital
Germany

To describe the technological background, the accuracy, and clinical feasibility for single session lung radiosurgery using a real-time robotic system with respiratory tracking. The latest version of image-guided real-time respiratory tracking software (Synchrony®, Accuray Incorporated, Sunnyvale, CA) was applied and is described. Accuracy measurements were performed using a newly designed moving phantom model. We treated 15 patients with 19 lung tumors with robotic radiosurgery (CyberKnife®, Accuray) using the same treatment parameters for all patients. Ten patients had primary tumors and five had metastatic tumors. All patients underwent computed tomography-guided percutaneous placement of one fiducial directly into the tumor, and were all treated with single session radiosurgery to a dose of 24 Gy. Follow up CT scanning was performed every two months.

All patients could be treated with the automated robotic technique. The respiratory tracking error was less than 1 mm and the overall shape of the dose profile was not affected by target motion and/or phase shift between fiducial and optical marker motion. Two patients required a chest tube insertion after fiducial implantation because of pneumothorax. One patient experienced nausea after treatment. No other short-term adverse reactions were found. One patient showed imaging signs of pneumonitis without a clinical correlation.

Single-session radiosurgery for lung tumor tracking using the described technology is a stable, safe, and feasible concept for respiratory tracking of tumors during robotic lung radiosurgery in selected patients. Longer follow-up is needed for definitive clinical results.

Key words: Cyberknife; Radiosurgery; Lung radiosurgery; and Image guided robotics.

Introduction

The preferred treatment for patients with non-small cell lung cancer (NSCLC) or single lung metastases from other cancers remains surgery. However, comorbidities, low performance status, poor lung function or previous surgery often prohibit additional surgical approaches, so alternative treatment options have to be selected. In most of these inoperable patients conventional radiation therapy, which can result in local control rates of 40-70%, or palliative chemotherapy is chosen (1-4). Conventional, conformal radiation therapy in the lung is made technically difficult by the substantial and variable target motion in this organ. Often the total dose needed to destroy the cancerous tissue cannot be fully applied while protecting the surrounding healthy tissue. This problem has been addressed in a number of ways, including immobilizing the patient using body frames and abdominal

[*]Corresponding Author:
Alexander Muacevic, M.D.
Email: Alexander.Muacevic@cyber-knife.net

compression devices (5, 6). Recently, gating techniques have been developed that allow the treatment beam to be turned on when breathing brings the tumor to within a predefined range and turned off when it leaves this target range. Although each of these techniques has permitted substantial dose escalation, they also require considerable setup margins to assure that the tumor receives sufficient radiation. A consequence is that a significant amount of healthy tissue is irradiated. Accordingly, most published series on stereotactic lung radiotherapy report hypofractionated treatment regimes (5-7).

We believe that the aim of lung radiosurgery should be the same as the aim of brain radiosurgery, that is, to maximize radiation to the tumor and minimize radiation exposure to surrounding normal tissue and adjacent critical structures. The newly developed respiratory tracking system that is a feature of the CyberKnife® System (Synchrony® Respiratory Tracking, Accuray Incorporated, Sunnyvale, CA) should allow achievement of this goal. The integrated imaging system coupled to the robotically controlled linear accelerator is designed to precisely and dynamically track moving targets such as pulmonary tumors. It is the purpose of the current paper to describe this new technology, present data on its accuracy in end-to-end phantom tests, and describe its clinical application using a stringent and minimally invasive setup for selected patients with NSCLC or pulmonary metastases.

Material and Methods

Radiosurgery System

The CyberKnife robotic radiosurgery system consists of a 6-MV compact linear accelerator (LINAC) mounted on a computer-controlled six-axis robotic manipulator. Integral to the system are orthogonally positioned x-ray cameras that acquire images during treatment. The images are processed automatically to identify radiographic features, and are registered to the treatment planning study to measure the position of the treatment site in real time. The system adapts to changes in patient position during treatment by acquiring targeting images repeatedly and adjusting the direction of the treatment beam accordingly. The treatment beam can be directed from hundreds of angles anterior and lateral to the patient.

Respiratory Motion Compensation

In order to compensate for tumor motion in the lung, it is necessary to know the internal position of the target throughout treatment. At any given time, the stereo X-ray system can acquire images to establish the tumor position (Fig. 1). Conventionally, small gold fiducials implanted in the proximity of the target are identified in both images and used to compute the 3D target position. While this provides accurate information on the tumor location at the instant the X-rays are taken, this is not sufficient to obtain real-time motion information. In the present system, the position of the chest is measured continuously by an external camera array that tracks the position of infrared markers on the patient's chest, and the location of the tumor is detected periodically in the x-ray images. A series of internal and external position measurements taken at the same time is used to establish a correlation model (Fig. 2). Throughout treatment, occasional measurements of both positions are used to check and update the model.

The correlation model allows the internal tumor position to be estimated based on the external marker position. Because the frequency of the external camera system is approximately 30 Hertz, this estimation can occur almost continuously while keeping the diagnostic X-ray dose low. Nevertheless, data processing and robot motion cause a time lag Δt. While this lag is small, it can be handled based on the cyclic nature of respiratory motion. At each time step t_i, the position of the tumor at time $t_i + \Delta t$ is computed. The robot is then controlled such that the beam will always point to the tumor (8-10).

Phantom Accuracy Tests

Commissioning and quality assurance of the Synchrony system is accomplished by using a phantom that contains fiducial markers and an orthogonal set of films, all mounted on a motion table that simulates target and external motion. The phantom consists of a precisely machined solid water cube with an acrylic ball (diameter 31.75 mm), which simulates the treatment target, inserted in the center. The cube consists of four pieces that can be disassembled to insert and align perpendicularly two self-developing radiochromic films (Gafchromic MD-55; International Speciality Products, Wayne, NJ, USA); thus, dose distributions in two orthogonal planes can be assessed simultaneously. The cube contains five radioopaque gold markers necessary for the target tracking. In order to provide isotropic scatter conditions the cube is inserted in a spherical cover.

During tests the phantom was placed on the motion table, which simulates superior-inferior tumor motion throughout the breathing cycle, similar to that reported by Shirato *et al*. (11). A single shaft with a dual cam drives the target platform and provides about 25 mm linear motion and a $\sin^3$ waveform, and also drives the platform for the external optical markers. A phase difference between the external marker motion and the phantom motion can be introduced by adjusting the second cam, which permits phase angles ranging from 0º to ± 180º.

Based on an axial CT scan of the phantom (slice thickness 1.2 mm) an isocentric treatment plan using the 25 mm collimator was generated covering the acrylic ball with a dose of 21 Gy prescribed to the 70% isodose line. The phantom was

Figure 1: Actual clinical system including the robot arm pointing the 6 MV LINAC to the target. Real-time image guidance based on 6D X-ray imaging (cameras mounted on ceiling, detectors to either side of the treatment couch) provides for frameless radiosurgery applications. The patients is positioned on a robotic patient couch.

placed and aligned with the motion table on the treatment couch. The speed control of the motion table was set to about 15 cycles per minute and the cam was adjusted to a phase shift of 0º. After generating a "respiration model" covering all portions of the motion cycle the phantom was irradiated according to the treatment plan. Using the same dose plan this test is repeated for phase shift angles of 10º, 20º, and 30º, respectively. A static test (no motion) serves as a reference. In addition, to illustrate the effects of motion compensation, one test was performed in which a static treatment was delivered to the moving phantom.

Figure 2: Figure showing actual traces of the chest motion from the IR marker and the tumor motion from the x-ray imaging system from a lung patient during treatment. A correlation model is established (middle row) mapping the frequently measured external marker position (upper row, tracking markers) to the infrequently measured internal marker position.

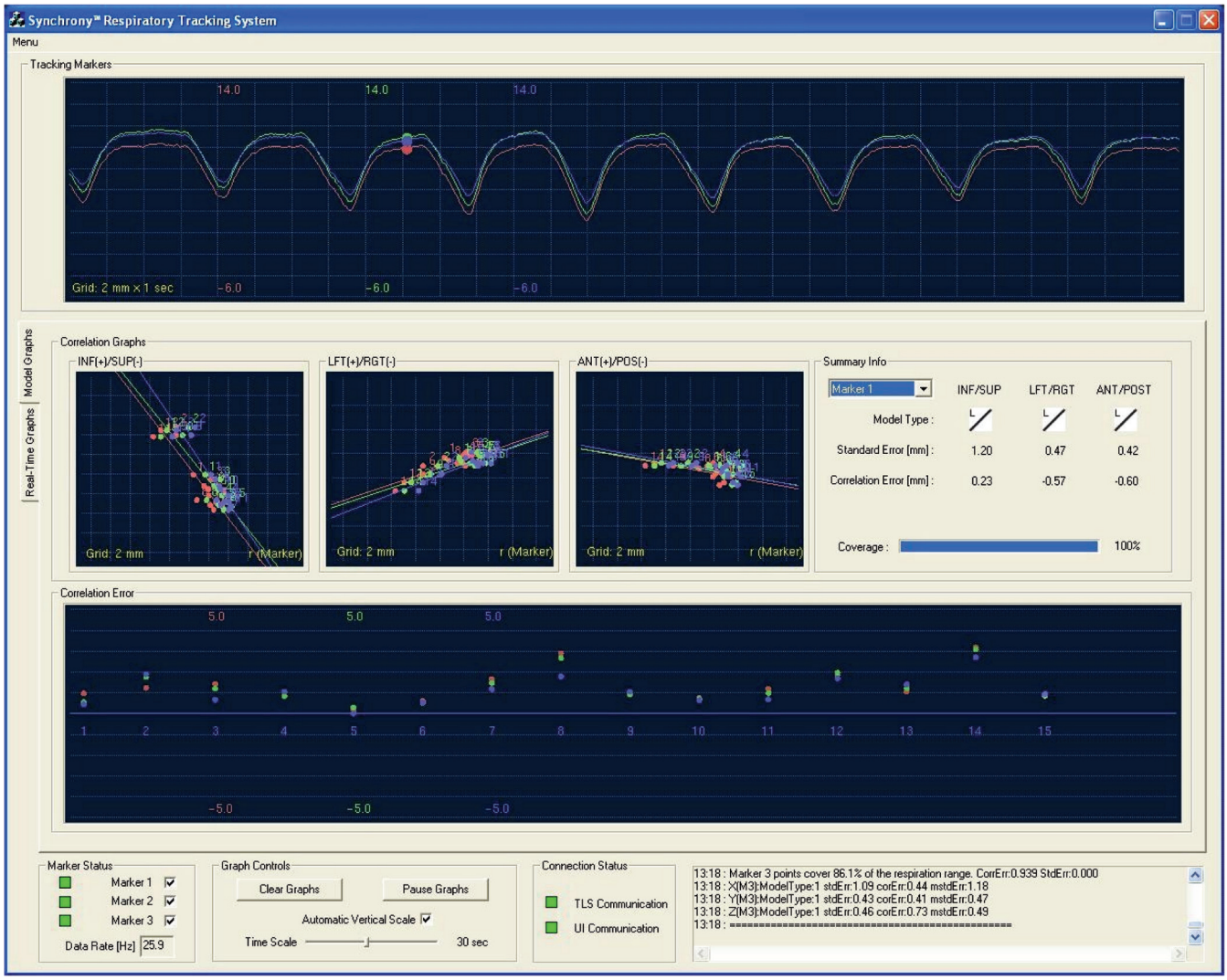

An optical density-to-dose calibration was obtained by irradiating film from the same batch in a solid water phantom under reference conditions (focus-to-film distance 80 cm, depth equivalent to 1.5 cm of water, and 60 mm circular field) from 5 Gy to 30 Gy in 5 Gy steps.

The irradiated films were removed from the phantom and scanned with a calibrated optical scanner after 24 hours allowing the film to stabilize. Targeting accuracy was evaluated using an end-to-end test analysis software tool. Additionally dose profiles in the direction of the motion (superior-inferior) were compared to the DICOM dose output of the treatment planning system. The slope of the high-dose gradient region, between 20% and 80% of the maximum dose, was determined as a measure of dose distribution spread in relation to an increasing phase shift.

Table I
Patient series.

Case number	Sex	Age	Pathology	TuVol cc	Prescribed dose	Prescription isodose (%)	V10Gy cc
1	M	46	Melanoma Metastasis	56	24	75	223.8
2	F	87	Ovarial Ca Metastasis	39	24	75	213.2
3	M	74	NSCLC	5.4	24	75	37.15
4	M	67	NSCLC	4.8	24	75	31.54
5	F	59	NSCLC	2.3	24	75	14.54
6	M	22	Seminoma Metastasis	1.5	24	75	9.89
7	F	57	NSCLC	12.4	24	75	26.96
8	M	66	NSCLC	15.8	24	75	130.5
				4.1	24	75	
9	M	59	NSCLC	26.8	24	75	145
10	M	54	Tonsillar Ca	21.9	24	75	107.6
			Metastasis	41.6	24	75	233
				29.9	24	75	132.3
				22.6	24	75	180
11	F	62	NSCLC	17.2	24	75	122
12	M	56	NSCLC	8.1	24	75	56.11
13	F	71	Colon Ca Metastasis	64.2	24	75	255.7
14	F	77	NSCLC	23.5	24	75	58
15	M	68	NSCLC	11.3	24	75	75

Targeting accuracy was evaluated by assessing the displacement of the symmetrical dose profile from the center position for all three orthogonal axis. This is assessed and calculated by the Accuray End-to-End test analysis software tool. The tracking error is defined as the length of the displacement vector

$$(tracking\ error = \sqrt{(dev_{Sup\text{-}Inf})^2 + (dev_{Right\text{-}Left})^2 + (dev_{ant\text{-}post})^2}).$$

This value includes all uncertainties throughout the complete treatment process including CT imaging, treatment planning, data processing and transfer, image guided dose delivery as well as marker recognition, and optical signal processing. The main factor of the tracking error is the resolution of the imaging systems involved (CT and Cyberknife digital imagers).

Patients

Fifteen patients were treated for 19 lung tumors with radiosurgery (Table I). There were nine men and six women. The age range was 22 to 87 years (mean age: 66 years). Ten patients had primary lung tumors and five metastatic tumors. One patient underwent radiosurgery for four lesions and one for two lesions. All others were treated for a single tumor. We only selected patients with a maximal tumor diameter of 3.5 cm. No patient underwent prior conventional radiation therapy for the targeted lesion. Tumor volume ranged from 1.5 to 64 cc (mean: 22 cc).

All patients were evaluated by a thoracic surgeon, a radiation oncologist and an interventional radiologist for eligibility of treatment and fiducial placement. All patients received one percutaneously implanted gold fiducial into the tumor using a pre-loaded 19-gauge needle under CT guidance and local anesthesia. No immobilization device was used during treatment. Patients underwent a contrast-enhanced CT scanning through the entire thoracic cavity using 1 mm thick slices. The treating surgeon and the radiation oncologist identified the location of the tumor and a radiosurgical treatment plan was developed using a nonisocentric, inverse-planning algorithm. The tumor was outlined in sequential axial CT images. The PTV was defined as the CTV, *i.e.*, no margins were applied. In order to reduce setup error patients were first aligned to the nearest vertebra to the tumor using fiducial-free spinal registration software (Xsight™, Accuray Incorporated) (12). After this setup procedure the lung treatment plan was loaded for treatment delivery. Modeling to correlate tumor motion (fiducial marker) and respiratory motion (LED on chest wall) was performed. We aimed to achieve a correlation error of less than 1 mm to start treatment. Radiation was then delivered in a single fraction using 24 Gy prescribed to the 75% isodose in all patients. If breathing patterns changed during the course of treatment, exceeding the recommended correlation error, remodeling was performed. Patients were followed clinically and radiographically after radiosurgery in 2-month intervals.

Results

Respiratory Motion Compensation

All patients could be treated technically using the real-time respiratory tumor tracking technique. Our approach to im-

plant only one fiducial and to minimize the setup error by aligning the patient with the non-invasive spinal protocol proved to be feasible, safe, and well tolerated by the patient. Remodeling was necessary according to the breathing patterns of the patients. One-to-five remodeling procedures (mean 2) during the treatment cycle became necessary. The median treatment time was 1 hour 50 minutes (1.5-3 hours).

Phantom Accuracy Tests

The results from the end-to-end test analysis did not reveal a relation between total tracking accuracy and phase shift between fiducial and optical marker movement. Tracking accuracy varied between 0.6 mm and 0.2 mm, which is within the range of our regular quality assurance results for static tests. The superior-inferior error, which is most likely to be affected by the superior-inferior phantom motion, was not clearly relation to phase shift. The individual test results are listed in Table II. Motion range was 25 mm (maximum motion with current motion table). The test was intended to test extreme scenario, as there is no significant difference between no motion and maximum motion. The system allows tracking in a range of +/- 25 mm in all directions. Excursions larger than this will trigger an interlock during imaging. During the treatment motions up to +/- 45 mm (*e.g.*, caused by a very deep breath) are tracked by the Synchrony system.

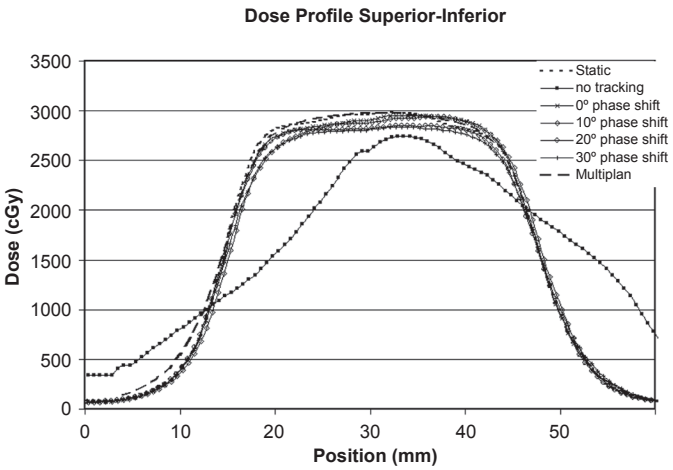

Figure 3: Dose profiles in the superior-inferior plane resulting from the end-to-end test targeting a sphere. In comparison to the calculated output of the Multiplan treatment planning system the dose profiles for the static situation (no phantom movement) and the results for the moving target are displayed. The 'no tracking' case (moving phantom) is for illustrative purposes only.

After scanning the films the superior-inferior pixel value profiles were extracted. These profiles were converted to dose profiles and normalized using the ratio of the maximum dose of the plan profile and the experimental static profiles. Figure 3 shows the smoothed film data in comparison with the planning system dose output. For all experimental data

Table II
End-to-end targeting results.

Test	Left-right deviation (mm)	Superior-inferior deviation (mm)	Anterior-posterior deviation (mm)	Targeting error (mm)
Static (reference)	-0,1091	-0,1237	0,1235	0,206
0° phase shift	-0,1446	-0,1257	0,0576	0,200
10° phase shift	-0,1910	-0,4667	-0,3180	0,596
20° phase shift	0,0033	-0,0545	0,1133	0,126
30° phase shift	-0,5030	-0,2447	0,0219	0,560
30° phase shift including motion in all planes(*)	-0,4994	-0,1980	-0,1203	0,551
No tracking	0,2380	-5,1355	0,4642	5,162

Individual results of the targeting test listing deviations in all planes for a 25 mm superior-inferior target motion in dependence of the phase angle between marker and target motion. One test (*) additionally includes left-right and anterior–posterior motion of the target.

Table III
Dose Gradient and width of dose profile.

	Superior		Inferior		Average		
	mm	Gradient (cGy/mm)	mm	Gradient (cGy/mm)	Avg-Gradient	Avg radial distance	Width at 50% dose level (mm)
static	5.45	346.0183	6.47	291.4683	318.7433	5.96	33.4
0° phase shift	5.5	339.4909	6.5	287.2615	313.3762	6	33.35
10° phase shift	6.38	296.9906	6.8	278.6471	287.8188	6.59	33.34
20° phase shift	5.55	327.1351	6.7	270.9851	299.0601	6.125	33.95
30° phase shift	6.1	294.9836	7.3	246.4932	270.7384	6.7	33.65
Plan	6.8	262.9412	6.9	259.1304	261.0358	6.85	36.2

there was a very good agreement with the calculated dose profile. Only assessing the maximum dose reached in the plateau area the values are near 100% of the static case for the 0º and 10º case, and are reduced to about 95% of the static case for the 20º and 30º phase shifts.

The slope between the 80% and 20% relative dose values served as a measure for the dose gradient. Compared with the calculated average dose gradient of 262 cGy/mm, (which equates to a radial distance of 6.85 mm between the 20% and 80% dose value), the experimental results show averaged values between 318 and 270 cGy/mm (radial distance between 6 and 6.7 mm). We also determined the width of the profiles at the 50% dose level. Compared to the static case (33.4 mm wide) only the profiles for 20º and 30º phase shifts are slightly wider (by 0.55 mm and 0.25 mm, respectively). The exact obtained values are given in Table III. As expected, the profile obtained for the case in which no target tracking was applied does not reflect the desired dose distribution at all. The dose is smeared out over the range of the target movement. Values from this experiment are listed for illustrative reasons only.

Clinical Outcome

Two patients required a chest tube insertion after fiducial implantation because of pneumothorax. One patient experienced nausea after treatment and one suffered from a radiological but not clinically relevant pneumonitis four months after treatment. No other adverse events were noted.

Discussion

It is well known that tumors in the lung move significantly. The movement can be cranio-caudal and anterior-posterior. It has also been demonstrated that the shape of lung lesions can change with respiration (13, 14). This explains why simply applying margins around the tumor is not sufficient; the risk of missing the target and irradiating too much healthy lung tissue is high. The respiratory tracking capabilities of the current radiosurgery system overcome most of the obvious disadvantages of standard radiation therapy for lung tumors. The integration of image-guided robotics enables the patient to be treated without any fixation devices as the robot compensates for tumor movement. The system constantly tracks the lesion, detecting inaccuracies and correcting if indicated.

Phantom Tests

The phantom study is an idealistic case in which uniform breathing is simulated and no deformation of the target occurs. Nevertheless, it demonstrates the accurate functioning and calibration of all the components involved in treatment with the motion tracking and compensation option of the CyberKnife system: imaging hardware and software, the correlation model between external and internal targets, the prediction and tracking algorithm, and the mechanical tracking of the target by the robot. In this experimental setting, the tracking error was well below 1 mm and the overall shape of the dose profile was not affected by target motion and/or phase shift between fiducial and optical marker motion.

The dose profile was smeared out over the dose plateau region as the phase shift increased, thus reducing the maximum dose. The redistribution of dose, demonstrated dramatically in the case in which no motion compensation was applied, did not affect the slope and the width of the dose profile. Thus, the planned dose distribution was reproduced very well despite phase shifts.

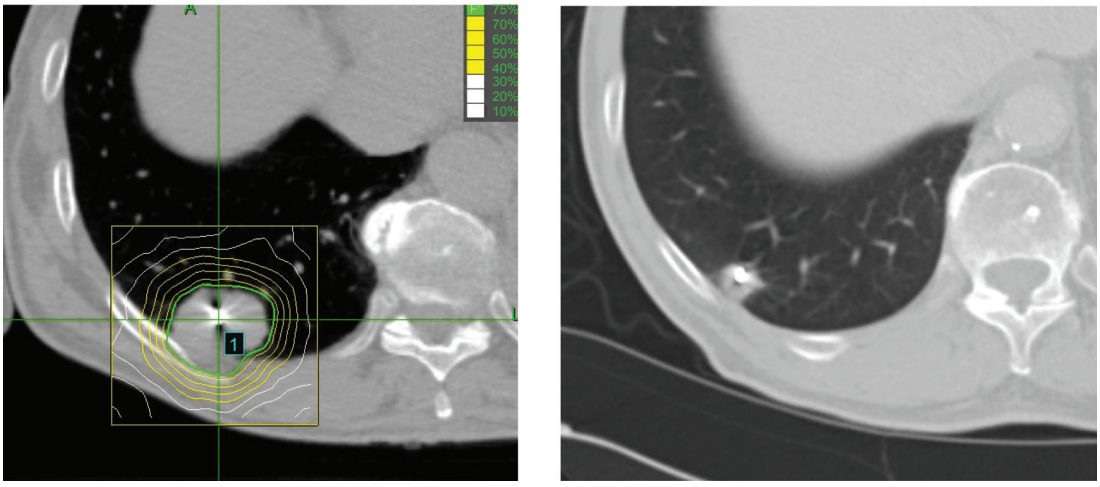

Figure 4: Figure shows a NSCLC lung tumor on the right side. A five mm gold seed fiducial was implanted percutaneously in the center of the tumor under CT guidance. The steep dose gradient of the isodoses and the prescription isodose covering the tumor without margins is displayed (left image). The follow up CT evaluation after two months showed a significant size reduction (right image).

Clinical Application

All selected patients could be treated with the described set-up in a single outpatient session. All patients were evaluated for feasibility of treatment by a multi-specialty team composed of thoracic surgeons, a radiation oncologist, a radiation physicist, and an interventional radiologist. It was decided to apply a homogeneous dose of 24 Gy to all patients prescribed to the 75% isodose. This single-dose approach differs from several other published approaches to stereotactic, high-dose radiation treatment in the lung. Timmerman *et al*. suggested a dose of 3 × 20 Gy for hypofractionated lung radiosurgery based on a phase I dose escalation study using an extracranial stereotactic body frame (15). He reported on one case of grade 3 pneumonitis and one case of grade 3 hypoxia. The concomitant prospective phase II trial confirmed the high local control rates using this treatment regime, although about 50% patients with central lung tumors experienced severe radiation toxicity during the 2-year follow-up time (16). Onishi *et al*. demonstrated encouraging results with a local failure rate of only 14.5% on a multi-institutional retrospective analysis of 245 patients treated by stereotactic radiation therapy with up to 22 fractions (7). Three published reports exist in which patients were treated with the CyberKnife for lung tumors. Only in the most recent one were all 20 patients treated with the latest version of the respiratory tracking system used in the present study (17). The majority of the patients in the Whyte and Le publication were treated using a breathhold technique (18, 19). None of these studies determined an optimal dose prescription. Whyte *et al*. delivered 15 Gy in a single session, and Le *et al*., in a follow-up study, added two groups of patients treated with single fractions of 25 Gy and 30 Gy. They found increased radiotherapy complications for doses greater than 25 Gy and a low 1-year local control rate (54%) for doses less than 20 Gy. Nuyttens *et al*. treated 20 patients applying 3 × 12 Gy, 3 × 15 Gy, and 3 × 20 Gy delivered every other day. Taking into account these findings and in order to overcome these highly heterogeneous dose prescription schemes we selected a stringent treatment algorithm in which 24 Gy was delivered single session to the 75% isodose level. We hypothesized that a technology providing high accuracy for moving targets should be capable of treating a lung tumor in a manner similar to the single-session treatment often employed for brain or spine tumors, without any margins surrounding the lesion. We aimed to reduce the dose to the healthy lung tissue as much as possible still giving enough dose to the pathological structures. This concept is feasible as long as the tumor is clearly visible on CT (Fig. 4). We suggest that this treatment regime be applied only to relatively small tumors (maximal diameter of 3.5 cm). The dose was well tolerated by all patients during short-term follow-up. Longer follow-up is needed for definitive clinical recommendations and risk estimations.

In order to reduce the invasiveness of the procedure to a minimum, we decided to only implant one fiducial into the lung tumor for image-guided tracking. Although one fiducial is generally regarded as not sufficient for 3-D tracking, we thought the risk of pneumothorax would be unacceptably high when implanting three fiducials or more into the lung. Furthermore, as we mainly treated small tumors, it would not have been feasible to implant three or four fiducial inside these tumors and fiducial markers placed in normal lung can easily migrate and are, therefore, unsuitable. To minimize the setup error and particularly the rotational error we did an automated setup as during spine radiosurgery, aligning the patient primarily to the vertebrae nearest to the lesion. After this setup we switched to the respiratory tumor tracking algorithm for creating the correlation model between tumor motion and the respiratory motion. This procedure was well tolerated by all patients.

Future Developments

Current research indicates that lung tumor tracking for peripheral tumors may be possible based on X-ray imaging alone. This may be realized with 4D CT imaging techniques and more sophisticated image processing and image registration techniques that automatically lock onto the tumor directly (10). This tracking innovation should enable clinicians to treat patients without implanting any fiducials, potentially making lung radiosurgery a completely non-invasive procedure.

Conclusion

The latest development of image-guided respiratory real-time tumor tracking for robotic lung radiosurgery is a technically safe and stable procedure. The tracking error is well below 1 mm and the overall shape of the dose profile is not affected by target motion and/or phase shift between fiducial and optical marker motion. The single-session radiosurgical procedure we applied showed excellent tolerability and seems to be a feasible treatment method for selected patients with small tumors. A longer follow-up and prospective evaluations are needed for definitive clinical results.

References

1. Dosoretz, D. E., Katin, M. J., Blitzer, P. H., Rubenstein, J. H., Galmarini, D. H., Garton, G. R., Salenius, S. A. Medically Inoperable Lung Carcinoma: The Role of Radiation Therapy. *Semin Radiat Oncol 6*, 98-104 (1996).
2. Graham, P. H., Gebski, V. J., Langlands, A. O. Radical Radiotherapy for Early Nonsmall Cell Lung Cancer. *Int J Radiat Oncol Biol Phys 31*, 261-266 (1995).
3. Jeremic, B., Classen, J., Bamberg, M. Radiotherapy Alone in Technically Operable, Medically Inoperable, Early-Stage (I/II) Non-Small-Cell Lung Cancer. *Int J Radiat Oncol Biol Phys 54*, 119-130 (2002).
4. Kaskowitz, L., Graham, M. V., Emami, B., Halverson, K. J., Rush, C. Radiation Therapy Alone for Stage I Non-Small Cell Lung Cancer. *Int J Radiat Oncol Biol Phys 27*, 517-523 (1993).

5. Blomgren, H., Lax, I., Naslund, I., Svanstrom, R. Stereotactic High Dose Fraction Radiation Therapy of Extracranial Tumors Using an Accelerator. Clinical Experience of the First Thirty-One Patients. *Acta Oncol 34*, 861-870 (1995).
6. Nagata, Y., Takayama, K., Matsuo, Y., Norihisa, Y., Mizowaki, T., Sakamoto, T., Sakamoto, M., Mitsumori, M., Shibuya, K., Araki, N., Yano, S., Hiraoka, M. Clinical Outcomes of a Phase I/Ii Study of 48 Gy of Stereotactic Body Radiotherapy in 4 Fractions for Primary Lung Cancer Using a Stereotactic Body Frame. *Int J Radiat Oncol Biol Phys 63*, 1427-1431 (2005).
7. Onishi, H., Araki, T., Shirato, H., Nagata, Y., Hiraoka, M., Gomi, K., Yamashita, T., Niibe, Y., Karasawa, K., Hayakawa, K., Takai, Y., Kimura, T., Hirokawa, Y., Takeda, A., Ouchi, A., Hareyama, M., Kokubo, M., Hara, R., Itami, J., Yamada, K. Stereotactic Hypofractionated High-Dose Irradiation for Stage I Nonsmall Cell Lung Carcinoma: Clinical Outcomes in 245 Subjects in a Japanese Multiinstitutional Study. *Cancer 101*, 1623-1631 (2004).
8. Schweikard, A., Glosser, G., Bodduluri, M., Murphy, M. J., Adler, J. R. Robotic Motion Compensation for Respiratory Movement During Radiosurgery. *Comput Aided Surg 5*, 263-277 (2000).
9. Schweikard, A., Shiomi, H., Adler, J. Respiration Tracking in Radiosurgery. *Med Phys 31*, 2738-2741 (2004).
10. Schweikard, A., Shiomi, H., Adler, J. R. Respiration Tracking in Radiosurgery without Fiducials. *Medical Robotics and Computer Assisted Surgery 1*, 19-27 (2005).
11. Shirato, H., Seppenwoolde, Y., Kitamura, K., Onimura, R., Shimizu, S. Intrafractional Tumor Motion: Lung and Liver. *Semin Radiat Oncol 14*, 10-18 (2004).
12. Muacevic, A., Staehler, M., Drexler, C., Wowra, B., Reiser, M., Tonn, J. C. Technical Description, Phantom Accuracy, and Clinical Feasibility for Fiducial-Free Frameless Real-Time Image-Guided Spinal Radiosurgery. *J Neurosurg Spine 5*, 303-312 (2006).
13. Wulf, J., Hadinger, U., Oppitz, U., Thiele, W., Flentje, M. Impact of Target Reproducibility on Tumor Dose in Stereotactic Radiotherapy of Targets in the Lung and Liver. *Radiother Oncol 66*, 141-150 (2003).
14. Wulf, J., Haedinger, U., Oppitz, U., Thiele, W., Mueller, G., Flentje, M. Stereotactic Radiotherapy for Primary Lung Cancer and Pulmonary Metastases: A Noninvasive Treatment Approach in Medically Inoperable Patients. *Int J Radiat Oncol Biol Phys 60*, 186-196 (2004).
15. Timmerman, R., Papiez, L., McGarry, R., Likes, L., DesRosiers, C., Frost, S., Williams, M. Extracranial Stereotactic Radioablation: Results of a Phase I Study in Medically Inoperable Stage I Non-Small Cell Lung Cancer. *Chest 124*, 1946-1955 (2003).
16. Timmerman, R., McGarry, R., Yiannoutsos, C., Papiez, L., Tudor, K., DeLuca, J., Ewing, M., Abdulrahman, R., DesRosiers, C., Williams, M., Fletcher, J. Excessive Toxicity When Treating Central Tumors in a Phase II Study of Stereotactic Body Radiation Therapy for Medically Inoperable Early-Stage Lung Cancer. *J Clin Oncol 24*, 4833-4839 (2006).
17. Nuyttens, J. J., Prevost, J. B., Praag, J., Hoogeman, M., Van Klaveren, R. J., Levendag, P. C., Pattynama, P. M. Lung Tumor Tracking During Stereotactic Radiotherapy Treatment with the Cyberknife: Marker Placement and Early Results. *Acta Oncol 45*, 961-965 (2006).
18. Le, Q. T., Loo, B. W., Ho, A., Cotrutz, C., Koong, A. C., Wakelee, H., Kee, S. T., Constantinescu, D., Whyte, R. I., Donington, J. Results of a Phase I Dose-Escalation Study Using Single-Fraction Stereotactic Radiotherapy for Lung Tumors. *Journal of Thoracic Oncology 1*, 802-809 (2006).
19. Whyte, R. I., Crownover, R., Murphy, M. J., Martin, D. P., Rice, T. W., DeCamp, M. M., Jr., Rodebaugh, R., Weinhous, M. S., Le, Q. T. Stereotactic Radiosurgery for Lung Tumors: Preliminary Report of a Phase I Trial. *Ann Thorac Surg 75*, 1097-1101 (2003).

Received: February 28, 2007; Revised: June 13, 2007; Accepted: June 22, 2007